Regional Moment Tensor Solutions for Source-Type Identification: The Crandall Canyon Mine Collapse

Douglas Dreger *(Berkeley Seismological Laboratory),* **Sean Ford** *(Lawrence Livermore National Laboratory),* **William Walter** *(Lawrence Livermore National Laboratory)*

Seismic moment tensor methods are now routinely applied at many scales from the study of micro-earthquakes to the characterization of damaging great earthquakes, and applied at regional distances they are proving to be a reliable tool for distinguishing between earthquakes and events associated with volcanic processes [*e.g. Dreger et al., 2000*], and other man-made sources of seismic radiation such as from explosions, or mining activity [*e.g. Ford et al., 2009*]. On August 6, 2007 a magnitude 3.9 seismic event was associated with the tragic collapse of a Utah coal mine. The event was well recorded by UUSS, USGS, and Earthscope USAarray stations (Fig. 1) The moment tensor inversion of complete, three-component, low-frequency (0.02 to 0.10 Hz) displacement records recovers a mechanism that is most consistent with the gravity driven vertical collapse of a horizontally oriented underground cavity (Fig. 1a). The seismic moment tensor of the event, is comprised 78% from a closing horizontal crack and a secondary 22% non-crack component, which results from the fitting of the large amplitude Love waves that were observed on the tangential component (Fig. 1c). Plausible interpretations of the secondary source include sympathetic vertical dip-slip faulting, non-uniform crack closure, and elastic relaxation in response to the mine collapse [*Ford et al., 2008*]. The moment tensor solution produces a pure dilatational P-wave first-motion mechanism consistent with the P-wave polarity observations [Pechman et al., 2008]. The source-type diagram [*Hudson et al., 1989*] in Fig. 1a illustrates the deviation from a pure earthquake double-couple (DC) source at the center in terms of a volumetric component (explosion or implosion) on the ordinate, and deviatoric component in terms of a volume compensated linear vector dipole (CLVD) on the abscissa. The mine-collapse event plots in the region of a negative or closing crack similar to solutions obtained for other mine and Nevada Test Site (NTS) cavity collapses [*Ford et al., 2009*]. The application of seismic moment tensor analysis to non-tectonic seismic events such as buried explosions or underground collapses as illustrated here, demonstrates the feasibility of continuous monitoring of regional distance seismic wavefields for source-type identification useful for nuclear explosion monitoring and possible emergency response.

References

Dreger, D. S., H. Tkalcic, and M. Johnston (2000). Dilational processes accompanying earthquakes in the Long Valley Caldera, *Science, 288,* 122-125.

Ford, S., D. Dreger and W. Walter (2008). Source Characterization of the August 6, 2007 Crandall Canyon Mine Seismic Event in Central Utah, *Seismol. Res. Lett., 79,* 637-644.

Ford, S. R., D. S. Dreger, and W. R. Walter (2009), Identifying isotropic events using a regional moment tensor inversion, *J. Geophys. Res., 114,* B01306.

Acknowledgements: We acknowledge DOE BAA contract DE-FC52-06NA27324 (BSL) and Contract W-7405-Eng-48 (LLNL) for support of this work.

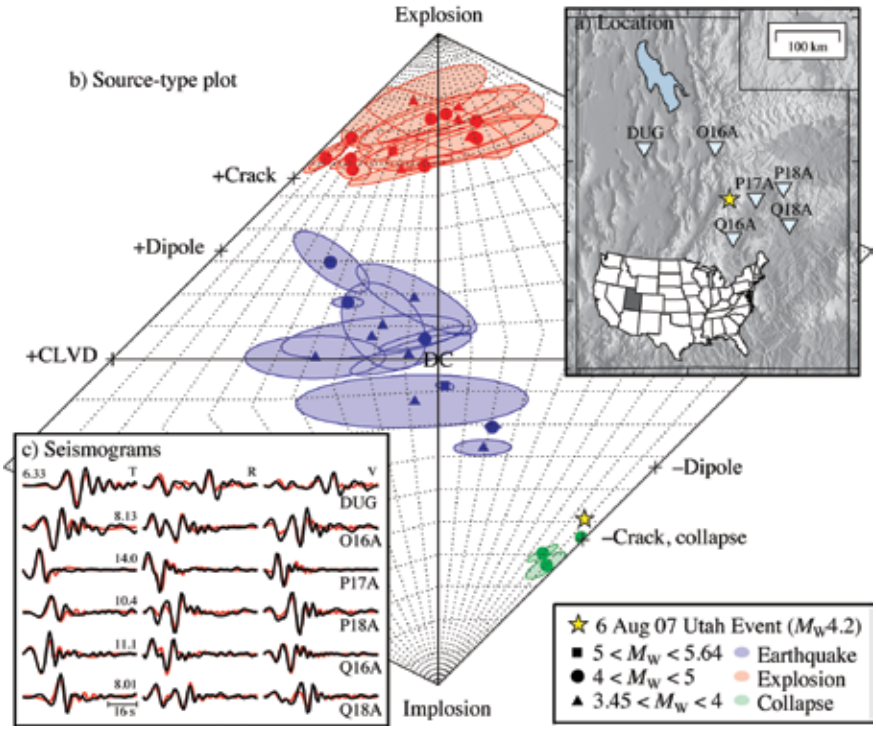

Fig 1. A) Source type plot showing separation of earthquake, explosion and collapse (yellow star shows the 08/06/2007 mine-collapse event). B) Location of the 08/06/2007 mine-collapse event and the 6 closest stations. C) Observed (black) and predicted (red) displacement waveforms (0.02 to 0.1 Hz).

Source Analysis of the Memorial Day Explosion, Kimchaek, North Korea

Sean R. Ford *(Lawrence Livermore National Laboratory),* **William R. Walter** *(Lawrence Livermore National Laboratory),* **Douglas S. Dreger** *(Berkeley Seismological Laboratoy)*

We perform a series of source inversions for the 25 May 2009 (Memorial Day) North Korean seismic event using intermediate period (10-50s) complete waveform modeling using data housed at IRIS. An earthquake source is inconsistent with the data and the best-fit full seismic moment tensor is dominantly explosive (~60%) with a moment magnitude (Mw) of 4.5. A pure explosion solution yields a scalar seismic moment of 1.8e22 dyne-cm (Mw4.1) and fits the data almost as well as the full solution. The difference between the full and explosion solutions is the predicted fit to observed tangential displacement, which requires some type of non-isotropic (non-explosive) radiation. Possible causes of the tangential displacement are additional tectonic sources, tensile failure at depth, and anisotropic wave propagation. Similar displacements may be hidden in the noise of the 2006 event. Future analyses of this type could be used to identify and characterize non-earthquake events such as explosions and mine collapses.

References

Ford, S.R., D. Dreger, and W. R. Walter, Source analysis of the Memorial Day explosion, Kimchaek, North Korea, *Geophys. Res. Lett., 36* (L21304), 2009

Acknowledgements: We acknowledge DOE BAA contract DE-FC52-06NA27324 (BSL) and Contract W-7405-Eng-48 (LLNL) for suppor

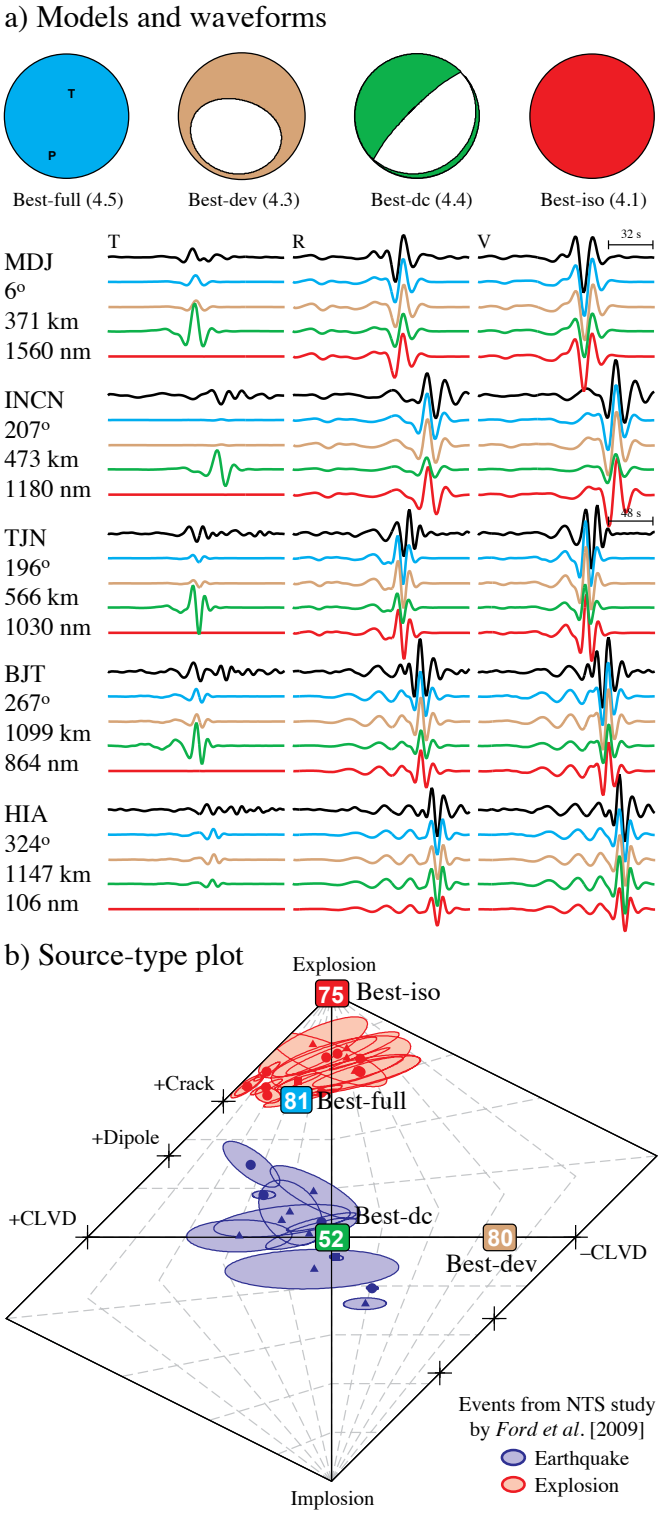

a) Models and their respective forward-predicted waveforms as a function of color compared with the actual waveforms (black line) all filtered between 10-50 sec period. b) Source-type plot with various solutions corresponding to the models given in a) and their associated fit percent.

Studying Earth's Wave Climate Using the Global Microseism

Richard Aster *(New Mexico Institute of Mining and Technology),* **Daniel McNamara** *(US Geological Survey, Golden, CO),* **Peter Bromirski** *(Integrative Oceanography Division, Scripps Institution of Oceanography, UC San Diego)*

Globally ubiquitous seismic background noise peaks, visible as broad peaks in seismic spectra with modes near 7 and 14 s period, are generated via two distinct mechanisms that transfer storm-generated gravity wave energy to the seismic wave field. Continuous digital ground motion data recorded by the Global Seismographic Network and precursor networks provide a unique integrative record of ocean wave to seismic coupling at regional to global scales [Aster et al., 2008] that can be applied to chronicle microseism power extreme events over hourly to decadal time periods. Because most land-observed microseism surface wave energy is generated at or near coasts [e.g. Bromirski et al., 1999], microseism metrics are particularly relevant to assessing changes in coastal ocean wave energy. For example, extreme microseism winter storm season event counts quantify the widespread wave influence of the El Nino Southern Oscillation (ENSO). The double-frequency (near 7 s) microseism is generated by interacting (standing wave) components of the ocean wave field, and is observed to be particularly volatile, likely both because of its quadratic dependence on wave height and because of its sensitivity to both incident wave angle and to coastal conditions that control ocean swell reflectivity. This suggests that the weaker single-frequency (near 14 s) microseism directly generated by ocean swell at coasts is a more representative seismic proxy for broad-scale ocean wave energy estimation. Metrics of extreme microseism events since the 1970s suggest slight positive trends in the northern hemisphere, and slightly declining trends in the Southern Hemisphere [Aster et al., 2010]. Microseism metrics are extendable to the pre-digital era through the digitization of analogue seismograms from long-running observatories, and thus offer the opportunity to quantify and characterize the wave influence of ENSO and other climate variations through to the early 20th century.

References

Aster, R., D.E. McNamara, and P. Bromirski (2008), Multi-decadal climate-induced variability in microseisms, *Seismol. Res. Lett., 79*, 194-202, doi:10.1785/gssrl.79.2.194.

Aster, R., D.E. McNamara, and P. Bromirski (2010), Global Trends in Extremal Microseism Intensity, *Geophys. Res. Lett*. in press.

Bromirski, P. D., R. E. Flick, and N. Graham (1999), Ocean wave height determined from inland seismometer data: Implications for investigating wave climate changes in the Northeast Pacific, *J. Geophys. Res.*, 104, 20,753-20,766.

Acknowledgements: The Global Seismographic Network is a cooperative scientific facility operated jointly by the Incorporated Research Institutions for Seismology, the United States Geological Survey (USGS), and the National Science Foundation. P. Bromirski has been supported in this research by the California Department of Boating and Waterways. Richard Boaz contributed significantly to database programming.

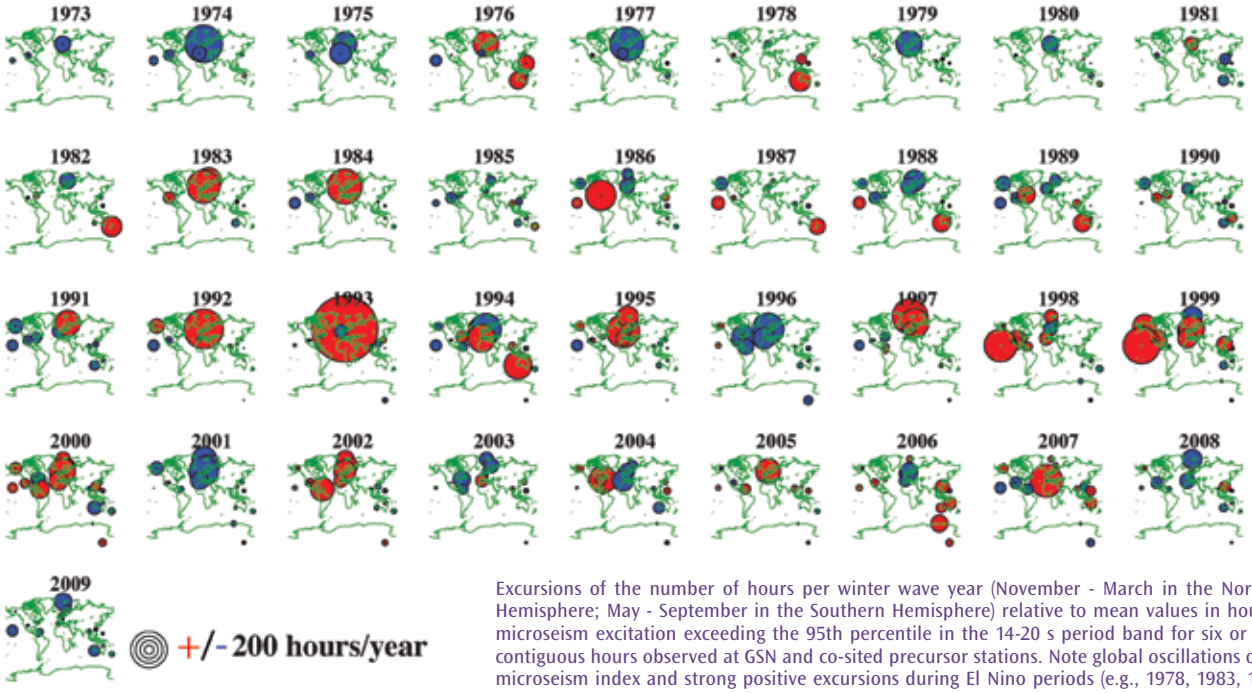

Excursions of the number of hours per winter wave year (November - March in the Northern Hemisphere; May - September in the Southern Hemisphere) relative to mean values in hours of microseism excitation exceeding the 95th percentile in the 14-20 s period band for six or more contiguous hours observed at GSN and co-sited precursor stations. Note global oscillations of this microseism index and strong positive excursions during El Nino periods (e.g., 1978, 1983, 1998). After Aster et al. (2010).

Iceberg Tremor and Ocean Signals Observed with Floating Seismographs

Richard Aster *(New Mexico Institute of Mining and Technology),* **Douglas MacAyeal** *(University of Chicago),* **Peter Bromirski** *(Integrative Oceanography Division, Scripps Institution of Oceanography, UC San Diego),* **Emile Okal** *(Northwestern University)*

Recent deployments of broadband seismometers atop Earth's largest floating ice bodies, the ice shelves and tabular icebergs of Antarctica have spurred the study of seismic and inertial phenomena associated with the dynamic (ocean tide- and ocean-wave-driven forcing) interaction of these bodies with the oceans, with the seafloor, and with each other. Harmonic and chaotic tremor-like signals generated by floating ice undergoing dynamic processes (collision and breakup) have been studied using both floating ice-deployed seismometry [*MacAyeal et al., 2008; Martin et al., 2010*] and by far-flung instruments at out to teleseismic/transoceanic distances. While much remains to be learned about the phenomenology and processes of these tremor sources and their impact on ice-body integrity, PASSCAL deployments in the Ross Sea region have shown that highly harmonic episodes of iceberg tremor are generated by extraordinarily sequences of repetitive stick-slip icequakes occurring at ice-ice contacts [*MacAyeal et al., 2008*], and that more chaotic signals, with some harmonic components, are generated during the grounding, during both breakup and nondestructive collisions [*Martin et al., 2010*]. Seismometers deployed atop floating ice further function as exquisitely sensitive buoys that can detect and characterize transoceanic swell, infragravity waves [*Cathles et al., 2009; Bromirski et al., 2010*], tsunamis [*Okal et al., 2006*], and regional ocean wave trains arising from calving icebergs [*MacAyeal et al., 2009*]. Recent work suggests that networks of seismometers on floating ice shelves can also uniquely measure repetitive ocean-driven strain fields that are projected to increase in frequency under climate change scenarios, and may contribute to the breakup of ice shelves [*Bromirski et al., 2010*].

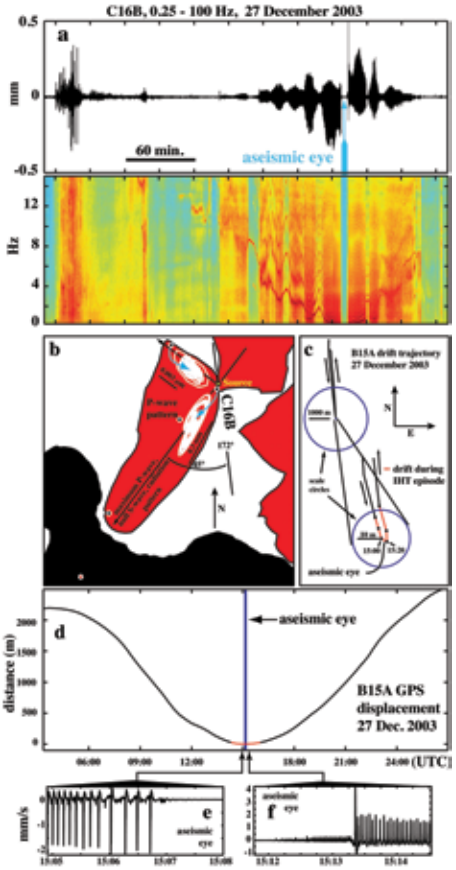

Iceberg tremor recorded by PASSCAL seismographs on iceberg C16 near Ross Island, Antarctica. a) Iceberg harmonic tremor (IHT) recorded bat C16B displayed as a vertical displacement seismogram and spectrogram; note the aseismic "eye". b) Map of station deployment, outline of Ross Island (black); icebergs (red); locations of C16 seismographs (white dots). White traces show particle motion at two stations (B and C) during IHT excitation; note quasi-P particle motion consistent with horizontal stick-slip motion between C16 and the moving B15A to the northwest. c) B15A GPS tidally-driven position relative to (the fixed) C16; lower graph shows a blowup showing reversing motion during IHT excitation (red). d) B15A GPS position showing the timing of the eye (a) and IHT tremor period (red). e and f) expanded view of seismogram showing repeating reversing stick-slip events due to the relative iceberg motions shown in (c) and (d); note polarity reversal as B15 motion reverses. After MacAyeal et al. [2008]

References

Bromirski, P., Sergienko, O., MacAyeal, D. (2010). Transoceanic infragravity waves impacting Antarctic ice shelves, Geophys. *Res. Lett., 37*, L02502, doi:10.1029/2009GL041488.

Cathles, L.M., Okal, E., MacAyeal, D. (2009). Seismic observations of sea swell on the floating Ross Ice Shelf, Antarctica, *J. Geophys. Res., 114*, F02015, doi:10.1029/2007JF000934.

MacAyeal, D. R., Okal, E., Aster, R., Bassis, J. (2008). Seismic and hydroacoustic tremor generated by colliding icebergs, J. *Geophys. Res., 113*, F03011, doi:10.1029/2008JF001005.

MacAyeal, D., Okal, E., Aster, R., Bassis, J. (2009). Seismic observations of glaciogenic ocean waves (micro-tsunamis) on icebergs and ice shelves, *J. Glaciology, 55*, 193-206, doi:10.3189/002214309788608679.

Martin, S., et al. (2010). Kinematic and seismic analysis of giant tabular iceberg breakup at Cape Adare, Antarctica, *J. Geophys. Res., 115*, B06311, doi:10.1029/2009JB006700.

Okal, E., MacAyeal, D. (2006). Seismic recording on drifting icebergs: Catching seismic waves, tsunamis and storms from sumatra and elsewhere, *Seismol. Res. Lett., 77*, 659-671, doi:10.1785/gssrl.77.6.659.

Acknowledgements: Instruments were provided by IRIS through the PASSCAL Instrument Center at New Mexico Tech. The Global Seismographic Network (GSN) is a cooperative scientific facility operated jointly by the Incorporated Research Institutions for Seismology, the USGS, and the National Science Foundation. All seismic data in this paper are available from the IRIS Data Management Center. Financial and logistical support was generously provided by the National Science Foundation under grants OPP-0229546, OPP-0229492, OPP- 0230028, OPP-0229305, and ANT-0538414.

Observations of Seismic and Acoustic Signals Produced by Calving, Bering Glacier, Alaska

Joshua P. Richardson *(Michigan Technological University),* **Gregory P. Waite** *(Michigan Technological University),*
Katelyn A. FitzGerald *(Michigan Technological University),* **Wayne D. Pennington** *(Michigan Technological University)*

Using short-period seismometers and small-aperture arrays of infrasound sensors, we recorded 126 calving and iceberg breakup events from the terminus of the Bering Glacier during five days in August 2008. The seismic signals were typically emergent, narrow-band, and lower-frequency (1-5 Hz), similar to seismic records from other glaciers, observed on a local scale [e.g. Qamar, 1988; O'Neel et al., 2007]. The acoustic records were characterized by shorter-duration, higher-frequency signals with more impulsive onsets. We demonstrate that triangular infrasound arrays permit improved locations of calving events over seismic arrivals that rely on a relatively complicated, poorly known, velocity model. We also discovered that a large percentage of events located away from the active calving face of the glacier and within Vitus Lake. The use of infrasound sensors proved extremely important in the differentiation of different parts of the source mechanism with one part propagating waves through the air and another propagating waves through the ground. Understanding the processes relating to ice-edge loss has serious implications in a changing climate, as fresh-water discharge has a significant impact on coastal currents within the Gulf of Alaska. [Richardson et al., 2010]

References

O'Neel, S., and W. T. Pfeffer (2007), Source mechanics for monochromatic icequakes produced during iceberg calving at Columbia Glacier, AK, *Geophys. Res. Lett., 34,* L22502.

Qamar, A. (1988), Calving icebergs: A source of low-frequency seismic signals from Columbia Glacier, Alaska, *J. Geophys. Res., 93*, 6615–6623.

Richardson, J. P., G. P. Waite, K. A. FitzGerald, and W. D. Pennington (2010), Characteristics of seismic and acoustic signals produced by calving, Bering Glacier, Alaska, *Geophys. Res. Lett., 37*, L03503.

Acknowledgements: The seismic instruments were provided by the Incorporated Research Institutions for Seismology (IRIS) through the PASSCAL Instrument Center at New Mexico Tech. Data collected will be available through the IRIS Data Management Center. The facilities of the IRIS Consortium are supported by the National Science Foundation under Cooperative Agreement EAR-0552316, the NSF Office of Polar Programs, and the DOE National Nuclear Security Administration. We would also like to thank the Michigan Tech Remote Sensing Institute, the Michigan Tech Office of the Vice President for Research, and the Michigan Tech Fund for their financial support.

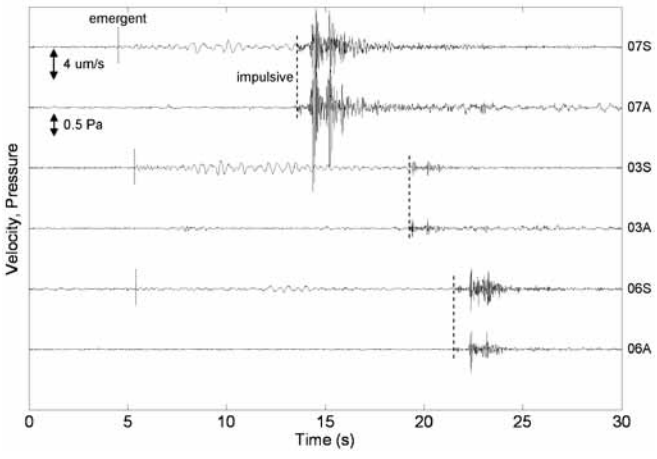

Vertical seismic (S) and coincident acoustic (A) traces recorded at each site from a single calving event on 07 August 2008 at 08:06 UTC. [Richardson et al., 2010]

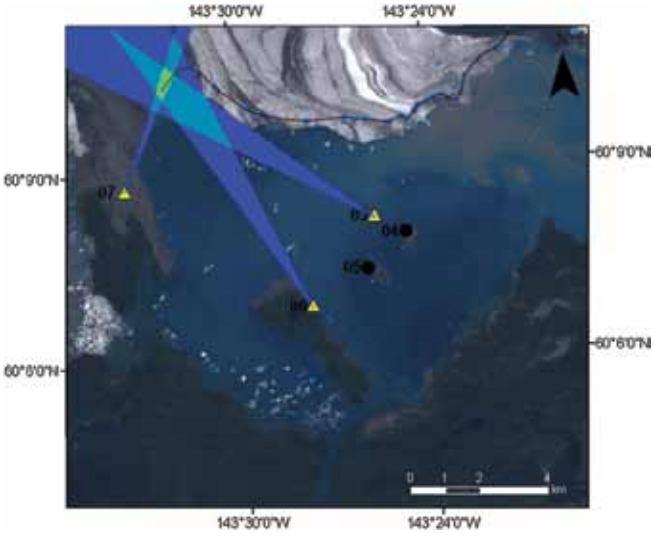

An example of the resulting solution produced by the intersection of three 99.7% confidence wedges at each array. [Richardson et al., 2010]

Elucidating the Stick-Slip Nature of the Whillans Ice Plain

Jacob Walter *(University of California, Santa Cruz),* **Emily E. Brodsky** *(University of California, Santa Cruz),* **Slawek Tulaczyk** *(University of California, Santa Cruz),* **Susan Y. Schwartz** *(University of California, Santa Cruz)*

The Whillans Ice Plain (WIP) is an approximately 200 km x 100 km x 600 m portion of the West Antarctic Ice Sheet that slips up to 0.5 m over a duration of 30 minutes, twice daily. Such bi-daily, tidally modulated stick-slip speed-ups provide insight into glacier dynamics and may be a unique analogue to tectonic earthquake/slow slip rupture. We deployed a network of continuously-operating GPS receivers in 2007 and operated on-ice broadband seismometers (partially provided by PASSCAL) during the austral summer of 2008 on WIP. Previous work during the 2004 field season suggested that these speed-ups initiate as failure of an asperity on or near "Ice Raft A" that triggers rupture across the entire WIP [*Wiens et al., 2008*]. Our results for the 2008 field season locate the slip initiation farther to the south of this feature, closer to the grounding line and the southernmost extent of the Ross Ice Shelf. A strong correlation between the amplitude of seismic waves generated at the rupture front and the total slip achieved over the duration of the slip event (~ 30 min) suggests slip-predictable behavior [Walter et al., submitted] or the ability to forecast the eventual slip based on the first minute of seismic radiation. Arrival time information compiled from stations QSPA and VNDA (continuous seismic data archived and provided by the IRIS DMC) show that successive slip events propagate with different rupture speeds (100-300 m/s) that strongly correlate (R-squared = 0.73, p-value = 0.0012) with the recurrence interval. In addition, the amount of slip achieved during each event appears to be correlated with the rupture speed. Our work suggests that the far-field transmission of seismic waves from glacier action is not dependent upon bulk ice movement, but rapid basal stress changes [*Walter et al., submitted*]. The availability of on-ice broadband seismometers and data at stations QSPA and VNDA yield important information regarding mechanics and dynamics of ice stream beds at the scale of 10s to 100s of km. Subglacial processes are notoriously difficult to constrain on these large scales, which are relevant to the understanding of regional and continental ice motion.

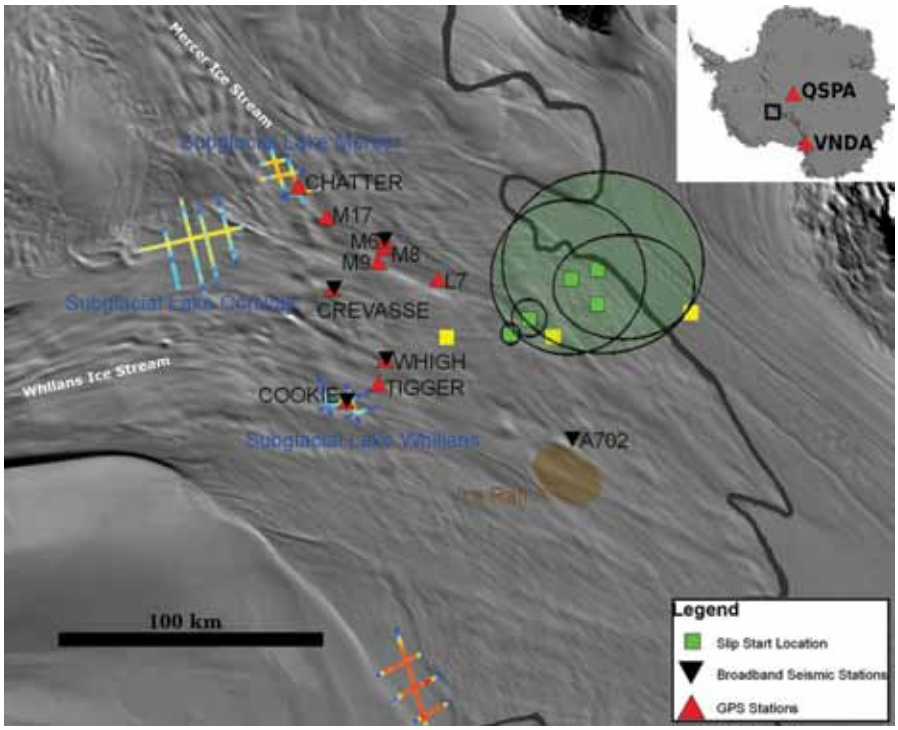

Station location map depicting continuous GPS network and broadband station names for the 2008 field season. Subglacial lake geometry is shown as IceSAT tracks, adapted from Fricker et al. [2007]. The green shaded circles 95% confidence level error ellipses encircling slip-start locations, shown as green squares. Yellow squares indicate slip-start locations with only three station observations.

References

Fricker, H. A., T. Scambos, R. Bindschadler (2007), An active subglacial water system in West Antarctica mapped from space, ***Science, 315***(5818): 1544-1548.

Walter, J. I., Brodsky, E. Tulaczyk, S., Schwartz, S., and R. Pettersson, submitted, Slip- predictability and dynamically fluctuating rupture speeds on a glacier-fault, Whillans Ice Plain, West Antarctica, ***J. Geophys. Res***. Earth Surface.

Wiens, D. A., S. Anandakrishnan, J. P. Winberry, and M. A. King (2008), Simultaneous teleseismic and geodetic observations of the stick-slip motion of an Antarctic ice stream, ***Nature, 453***: 770774.

Acknowledgements: This work was funded primarily by NSF Antarctic Sciences Division Grant number 0636970. Support for JW is provided by a NASA Earth and Space Science Fellowship. Some broadband seismic equipment was provided by PASSCAL. The IRIS DMC manages and archives data from stations QSPA and VNDA.

Infrasonic Imaging with the USArray

Kris Walker *(Laboratory for Atmospheric Acoustics, IGPP, SIO, Univ. of California, San Diego),* **Michael Hedlin** *(Laboratory for Atmospheric Acoustics, IGPP, SIO, Univ. of California, San Diego),* **Catherine de Groot-Hedlin** *(Laboratory for Atmospheric Acoustics, IGPP, SIO, Univ. of California, San Diego)*

The USArray directly measures ground motion, which can mostly be attributed to ocean waves, earthquakes, volcanoes, and weather systems that load the Earth's surface. Another source of ground motion is the transfer of atmospheric acoustic energy into seismic energy at the Earth's surface. Infrasound (low frequency sound below ~20 Hz) can travel great distances unattenuated in atmospheric ducts created by layers of slow sound speed. The infrasound wave field is rich due to a variety of anthropogenic and geophysical phenomena including earthquakes, volcanoes, landslides, meteors, lightning and sprites, auroras, and oceanic and atmospheric processes. Globally spaced microbarometer arrays with apertures of 100 m to 2 km are typically used to study these sources. However, these arrays are separated by thousands of kilometers, which places considerable limits on what they can teach us about infrasound source physics. The USArray is in a position to study infrasound sources in unprecedented detail. Array processing methods, such as reverse-time migration (RTM), may work well in automated detection and location of infrasound sources registered by the USArray (see also Hedlin et al. contribution). Hundreds of sources have been detected thus far using this technique. For example, below is a USArray "infrasonic image" of a Vandenberg Air Force Base rocket launch.

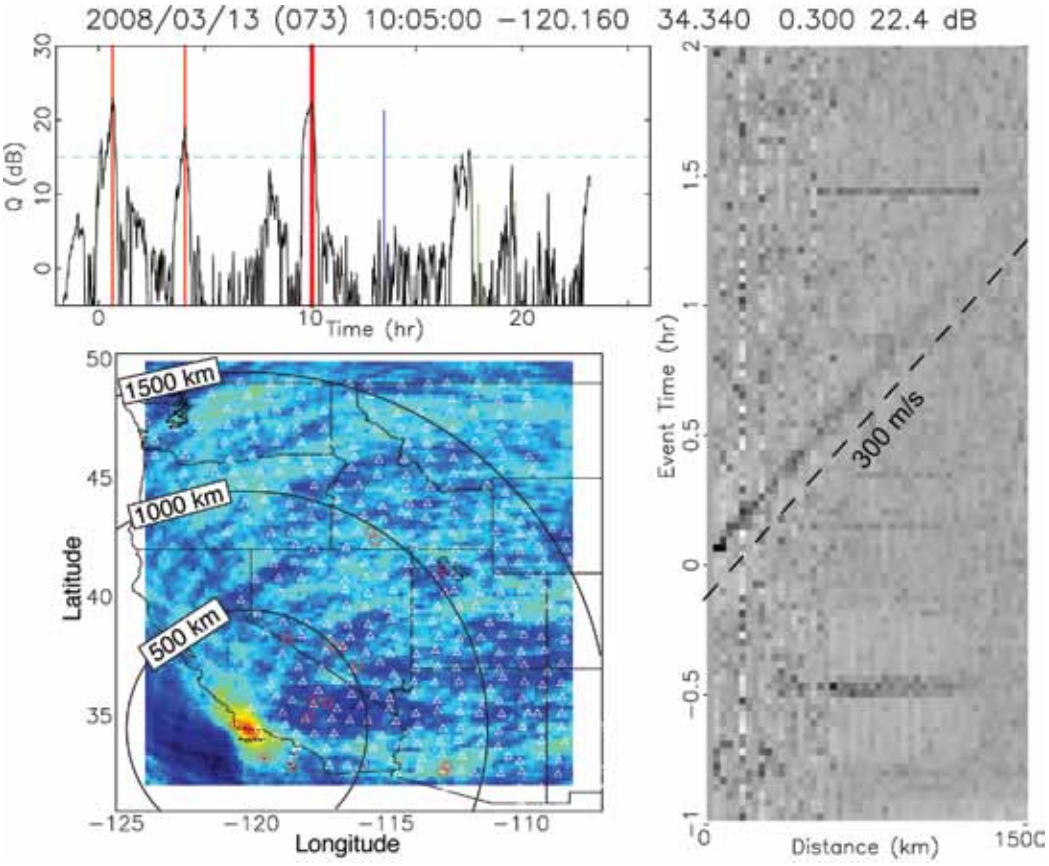

The detector function (upper left) images the source in time; there is a peak at the launch time (thick red line) with a signal-to-noise ratio of 22 dB. Other colored lines indicate known regional and teleseismic earthquake times. The map shows the seismic energy migrated back to the source, where it constructively interferes, imaging the source in space at the source time. The record section to the right shows that the migrated energy moves out at ~300 m/s, indicating that rocket infrasound is observed out to ~1500 km. Horizontally aligned signals are earthquakes.

Probing the Atmosphere and Atmospheric Sources with the USArray

Michael Hedlin *(Laboratory for Atmospheric Acoustics, U.C. San Diego),* **Kris Walker** *(Laboratory for Atmospheric Acoustics, U.C. San Diego),* **Catherine de Groot-Hedlin** *(Laboratory for Atmospheric Acoustics, U.C. San Diego),* **Doug Drob** *(Naval Research Laboratory)*

The USArray is designed to image the subsurface structure of the United States with exceptional resolution at a continental scale and for studies of regional and teleseismic earthquakes. Although the sensors of this network directly measure ground motion, they indirectly measure other phenomena that affect ground motion. It has been known for a long time that infrasound can be detected by seismometers through acoustic-to-seismic conversion at the ground/atmosphere interface. The USArray data archive contains recordings of several hundred large atmospheric events. One example is a bolide that burst above Oregon State on February 19, 2008 and was recorded by several hundred seismic stations and four infrasound arrays. The bolide source parameters were precisely determined by the seismic data, and the time-offset records show several phase branches corresponding to multiple arrivals. Such branches have never before been observed in such spectacular detail because infrasound arrays separated by thousands of kilometers are typically used for infrasound studies. The branches from such a large number of events occurring through the year are proving to be very useful for study of infrasound propagation and atmospheric structure.

Acknowledgements: We would like to acknowledge Earthscope and IRIS for data from the USArray without which this study would not have been possible. We would like to thank Matt Fouch at the University of Arizona and David James at the Carnegie Institution of Washington for giving us access to data from their High Lava Plains Seismic Experiment. We would also like to thank Gene Humphries at the University of Oregon for giving us access to data from the Wallowa Flexible Array Experiment. This article was made possible through support provided by US Army Space and Missile Defense Command. The opinions expressed herein are those of the authors and do not necessarily reflect the views of the US Army Space and Missile Defense Command.

USArray stations and regional infrasound arrays at the time of the bolide event.

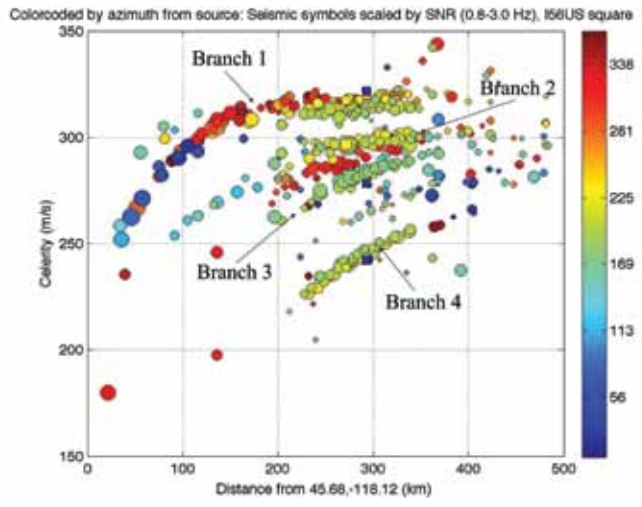

All branches from this event recorded by seismic stations and the infrasound array I56US. Symbols are scaled by SNR and colored by azimuth from the source. Signals from the lone infrasound array near the source are represented by the blue squares at 300 km.

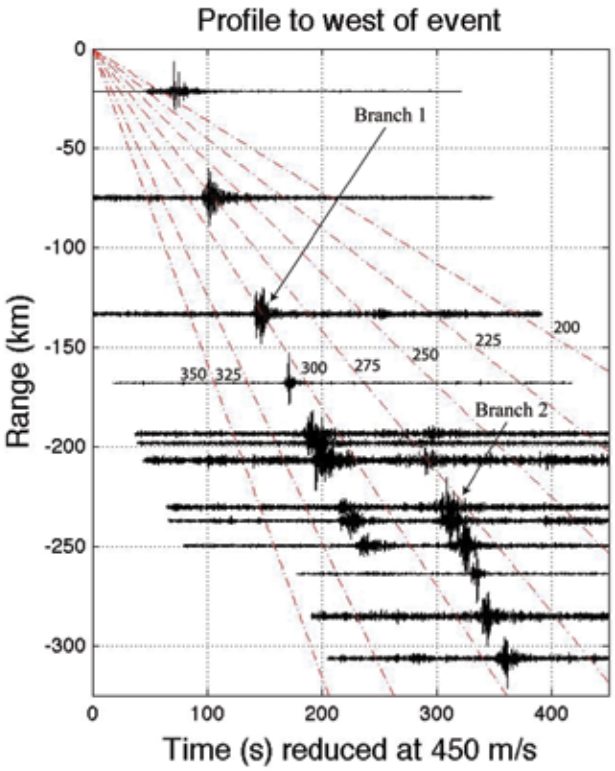

A record section to the west of the event. We see two acoustic branches (at celerities from 225 to 312 m/s) to a range of over 300 km in this direction.

Harmonic Tremor on Active Volcanoes: Seismo-Acoustic Wavefields

Jonathan Lees *(University of North Carolina, Chapel Hill),* **Jeffrey Johnson** *(New Mexico Institute of Technology)*

Harmonic tremor is often observed on active volcanoes where seismo-acoustic arrays are deployed. In this presentation we review characteristic observational phenomena and discuss the continuum from monochromatic, oscillatory behavior through periodic acoustic pulses (i.e. chugging) to spasmodic drumming on numerous volcanoes world wide. Harmonic tremor can provide detailed constraints on physical parameters controlling activity in active vents through physical modeling. These include physical constraints on the vent geometry, composition and density of the multiphase fluids, and visco-elastic parameters of choked flow in the conduits. Examples will show seismic tremor with and without an associated acoustic emission, an indicator of dynamic processes occurring at the top of the active vent. While explosive activity can range widely between volcanoes, harmonic tremor often exhibits remarkably similar behavior on vents as diverse as Karymsky, Tungurahua, Reventador, and Santiaguito Volcanoes. For example, chugging activity typically has a consistent 0.7-2 Hz signal on many volcanoes world wide. Commonly observed gliding, where frequency modulates over time, suggests that conditions in the conduit are non-stationary, and must be treated with specialized time series analysis tools. We explore these phenomena and highlight possible models explaining these near surface vent emissions.

References

Lees, J.M., Johnson, J.B., Ruiz, M., Troncoso, L. and Welsh, M., (2008). Reventador Volcano 2005: Eruptive Activity Inferred from Seismo-Acoustic Observation. *J. Volcanol. Geotherm. Res., 176*(1): 179-190, doi:10.1016/j.jvolgeores.2007.10.006.

Lees, J.M. and Ruiz, M., (2008). Non-linear Explosion Tremor at Sangay, Volcano, Ecuador. *J. Volcanol. Geotherm. Res., 176*(1): 170-178 doi:10.1016/j.jvolgeores.2007.08.012

Johnson, J. B., and J. M. Lees (2000), Plugs and Chugs – Strombolian activity at Karymsky, Russia, and Sangay, Ecuador, *J. Volcanol. Geotherm. Res., 101*, 67-82.

Acknowledgements: NSF: EAR-9614639 , "Side Edge of Kamchatka Slab", June 1, 1997-July 31, 2000. NSF Proposal No: EAR-0738768 Title: Co

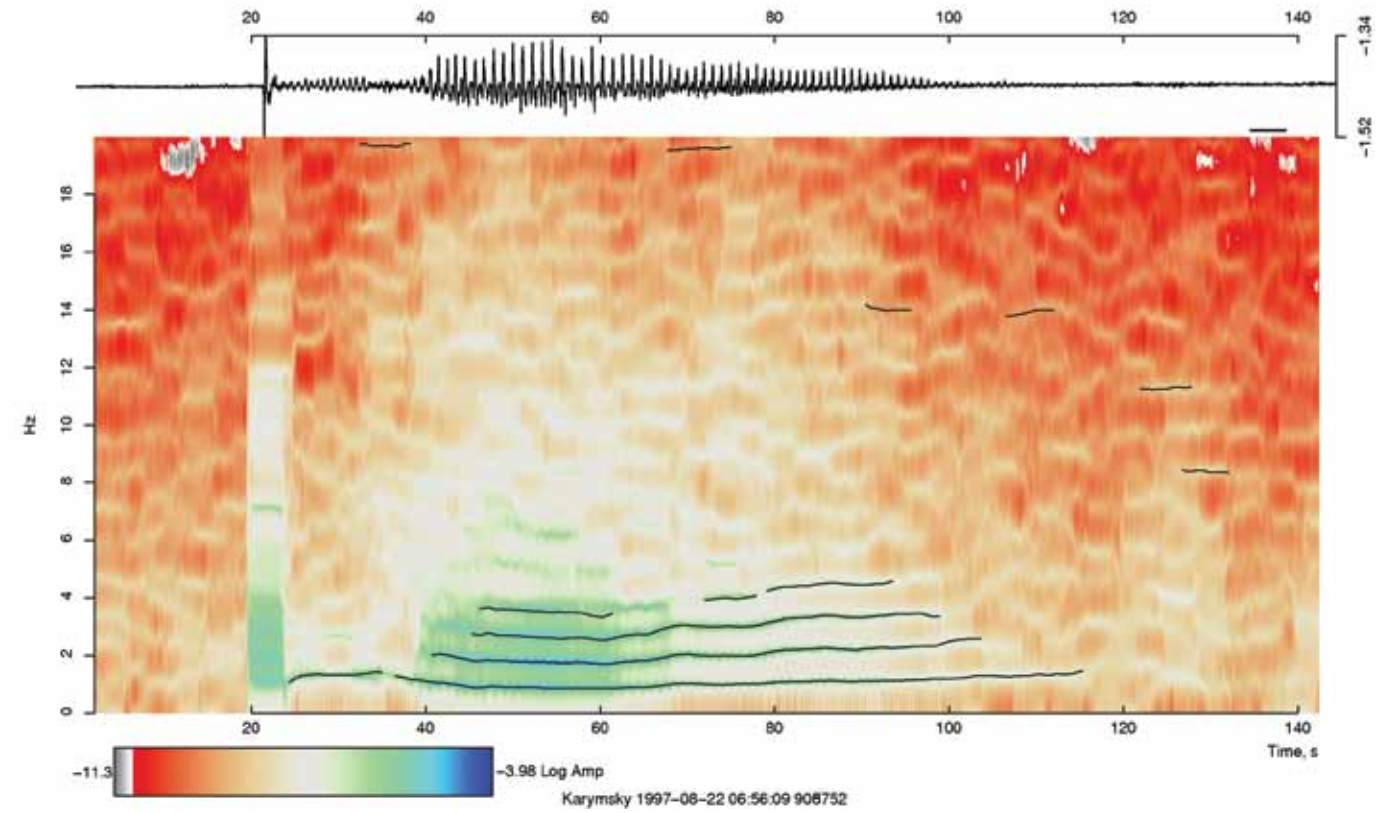

Spectrogram of Karymsky Volcano chugging, 1997. Lines represent the fundamental and possible integer harmonics of the chugging sequence.

Volcanic Plume Height Measured by Seismic Waves Based on a Mechanical Model

Stephanie Prejean *(Alaska Volcano Observatory, USGS),* **Emily Brodsky** *(UC Santa Cruz)*

In August 2008 an unmonitored, largely unstudied Aleutian volcano, Kasatochi, erupted catastrophically. Here we use seismic data to infer the height of large eruptive columns, like those of Kasatochi, based on a combination of existing fluid and solid mechanical models. In so doing, we propose a connection between common observable, short-period seismic wave amplitude, to the physics of an eruptive column. To construct a combined model, we estimate the mass ejection rate of material from the vent based on the plume height, assuming that the height is controlled by thermal buoyancy for a continuous plume. Using the calculated mass ejection rate, we then derive the equivalent vertical force on the Earth through a momentum balance. Finally, we calculate the far-field surface waves resulting from the vertical force. Physically, this single force reflects the counter force of the eruption as material is discharged into the atmosphere. We explore the applicability of the combined model to relatively high frequency seismic waves recorded at ~ 1 s. The model performs well for the 2008 eruption of Kasatochi volcano and the 2006 eruption of Augustine volcano. The consistency between the seismically inferred and measured plume heights indicates that in these cases the far-field 1 s seismic energy radiated by fluctuating flow in the volcanic jet during eruption is a useful indicator of overall mass ejection rates. Use of the model holds promise for characterizing eruptions and evaluating ash hazards to aircraft in real time based on far-field short-period seismic data.

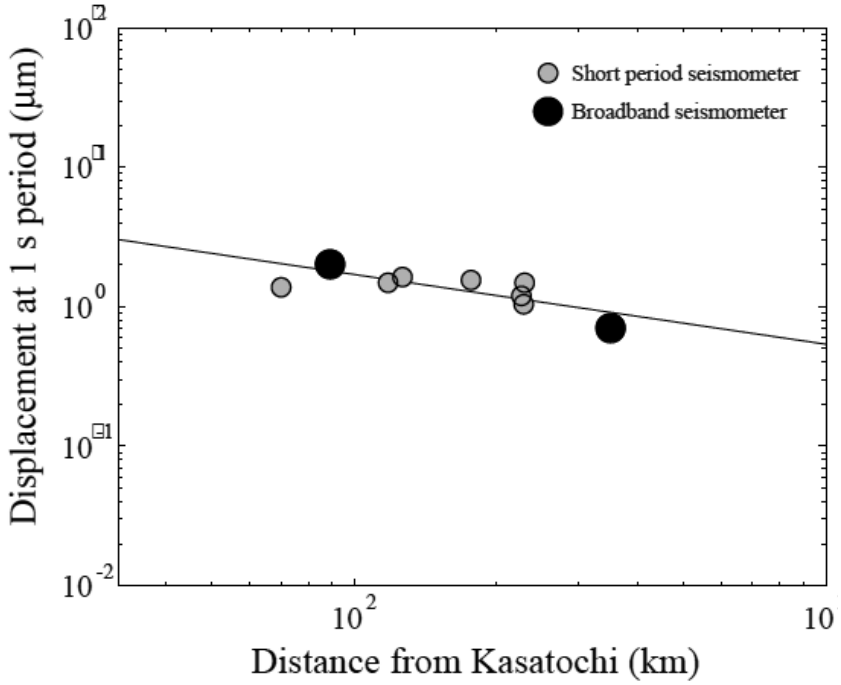

Ground displacement at 1 s period of co-eruptive seismicity with distance from Kasatochi volcano for the large ash producing explosion at 2008. Large dots are broadband stations ATKA and AMKA. Small dots are short-period stations. Preferred forward model fit shown with solid line.

Anomalous Earthquakes Generated by Collapse of Magma Chambers

Ashley Shuler, Göran Ekström *(Department of Earth and Environmental Sciences, Columbia University, Lamont-Doherty Earth Observatory)*

Recent advances in earthquake detection using intermediate period surface waves have resulted in the discovery of hundreds of earthquakes (Mw>4.5) that previously went unrecorded in global seismicity catalogs [Ekström, 2006]. Many of these events are located in areas with good station coverage, and may have escaped detection due to unusual source properties. A series of five such earthquakes were detected near Nyiragongo Volcano in the Democratic Republic of the Congo between 2002 and 2005. The first three events occurred several days after the massive fissure eruption of Nyiragongo in January 2002. The final two events occurred in 2003 and 2005, and are not linked to a major eruption in the region, but did occur as the level of Nyiragongo's summit lava lake was rising. This set of earthquakes is anomalous in two regards. First, these earthquakes are depleted in high-frequency energy over approximately 0.1 Hz, and can be considered slow earthquakes. Second, centroid-moment-tensor solutions indicate that these earthquakes are highly non-double-couple, each having a large compensated-linear-vector-dipole component of the moment tensor. This indicates that the double couple model for shear failure on a planar fault cannot explain the radiation pattern of these earthquakes. Drawing on models based on similar observations from other active volcanoes [Nettles and Ekström, 1998; Ekström and Nettles, 2002], we propose that the earthquakes are caused by slip on pre-existing, non-planar faults located beneath the edifice of the volcano. We suggest a mechanism in which these newly detected earthquakes are generated by the collapse of the roof of a shallow magma chamber along an inward-dipping cone-shaped ring fault [Shuler and Ekström, 2009]. As one might expect, these events can occur in association with an ongoing volcanic eruption. In the case of the first three earthquakes, diking events during the 2002 eruption reduced the pressure in a shallow magma chamber, leading it to collapse along the pre-existing ring fault. However, a similar mechanism can also explain the occurrence of these earthquakes due to the transport of magma from deeper to more shallow magma chambers. The earthquakes in 2003 and 2005 occurred during a period of lava lake level rise, and so are associated with magma ascent processes. The detection of this type of earthquake at other active volcanoes may be useful for inferring magma transport and determining the likelihood of future eruptions.

References

Ekström, G. (2006), Global Detection and Location of Seismic Sources by Using Surface Waves, *Bull. Seismol. Soc. Amer., 96*(4A), 1201-1212.

Shuler, A., and G. Ekström (2009), Anomalous earthquakes associated with Nyiragongo Volcano: Observations and potential mechanisms, *J. Volcanol. Geoth. Res., 181*(3-4), 219-230.

Nettles, M., and G. Ekström (1998), Faulting mechanism of anomalous earthquakes near Bárdarbunga Volcano, Iceland, *J. Geophys. Res., 103*(B8), 17,973-17,983.

Ekström, G. and M. Nettles (2002), Detection and location of slow seismic sources using surface waves, Eos Trans. AGU, 83(47), Fall Meet. Suppl., Abstract S72E-06.

Acknowledgements: The seismic waveforms used in this study were obtained from the GSN, GEOSCOPE, GEOFON, and MEDNET. Additional data from the Ethiopia and Kenya Broadband Experiments were also utilized (PI Andy Nyblade). The facilities of the IRIS Data Management System, and specifically the IRIS Data Management Center, were used for access to waveforms and metadata required in this study. The schematic diagram in Figure 1 was rendered by Liz Starin. This work was funded by National Science Foundation Award EAR-0639963. Ashley Shuler was also supported by an NSF Graduate Research Fellowship.

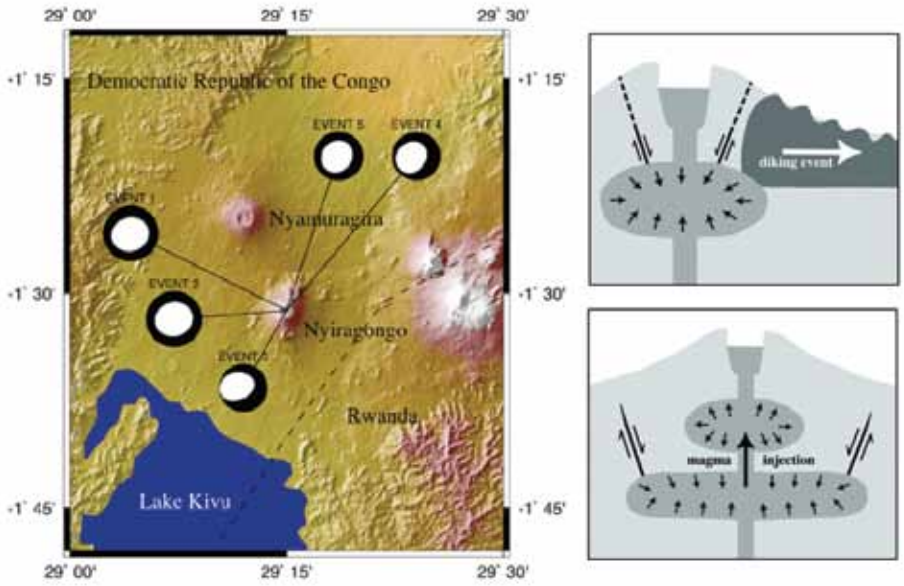

Focal mechanisms for newly detected earthquakes at Nyiragongo. Schematic diagram on right shows the physical mechanism for these events. Earthquakes are generated by slip on inward-dipping ring faults due to deflation of shallow magma chambers. This can be caused either by diking events during volcanic eruptions (top), or by the transport of magma from deeper to more shallow magma chambers (bottom).

Eruption Dynamics at Mount St. Helens Imaged from Broadband Seismic Waveforms: Interaction of the Shallow Magmatic and Hydrothermal Systems

Gregory Waite *(Michigan Technological University)*

The 2004-2008 eruption at Mount St. Helens was characterized by dome building and shallow, repetitive, long-period (LP) earthquakes. We analyzed the seismicity using a temporary array of 19 intermediate band PASSCAL seismometers deployed during the second half of 2005 from ~1 to 6 km from the active vent. Waveform cross-correlation of the LP events shows they were remarkable similarity for a majority of the earthquakes over periods of several weeks, indicating a repetitive source mechanism. Stacked spectra of these events display multiple peaks between 0.5 and 2 Hz that are common to most stations; this suggests the low-frequency waveforms are due to a source process, rather than path affects. When the first motions were discernible, they were dilatational on stations at all distances and azimuths. In addition to the LP events, lower-amplitude very-long-period (VLP) events commonly accompany the LP events. We modeled the source mechanisms of LP and VLP events in the 0.5 - 4 s and 8 - 40 s bands, respectively by full waveform inversion. The source mechanism of the LP events includes: 1) a volumetric component modeled as resonance of a gently NNW-dipping, steam-filled crack located directly beneath the actively-extruding part of the new dome and within 100 m of the crater floor and 2) a vertical single force attributed to movement of the overlying dome. The VLP source, which also includes volumetric and single-force components, is 250 m deeper and NNW of the LP source, at the SW edge of the 1980s lava dome. The volumetric component points to the compression and expansion of a shallow, magma-filled sill, which is subparallel to the hydrothermal crack imaged at the LP source, coupled with a smaller component of expansion and compression of a dike. The single-force components are due to changes in the velocity of magma moving through the conduit. The location, geometry and timing of the sources suggest the VLP and LP events are caused by perturbations of a common crack system.

References

Waite, G. P., B. A. Chouet, and P. B. Dawson (2008), Eruption dynamics at Mount St. Helens imaged from broadband seismic waveforms: Interaction of the shallow magmatic and hydrothermal systems, *J. Geophys. Res., 113*(B2), B02305.

Acknowledgements: Funding was provided primarily by the USGS Mendenhall Postdoctoral Fellowship. The IRIS-PASSCAL Instrument Center provided instruments and support for the temporary network. Data collected are available through the IRIS Data Management Center. The facilities of the IRIS Consortium are supported by the National Science Foundation under Cooperative Agreement EAR-0552316, the NSF Office of Polar Programs and the DOE National Nuclear Security Administration

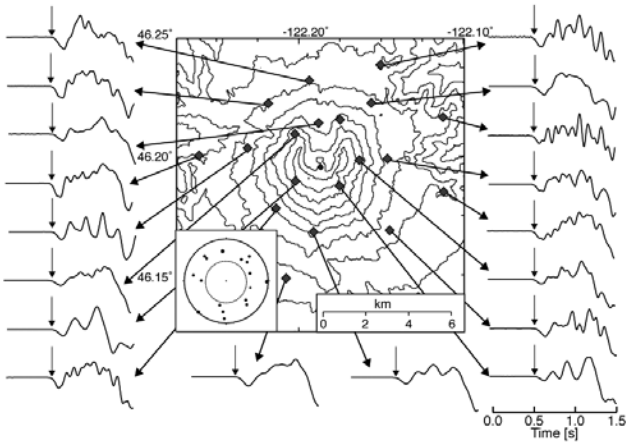

Figure 1. Dilatational first motions are clear at all of the broadband stations for a sample event from 31 July 2005, plotted as a circle in the crater. The focal sphere in the inset shows distribution of the first motion recordings for the broadband stations, with a dashed line in the middle outlining the region where there are no broadband stations.

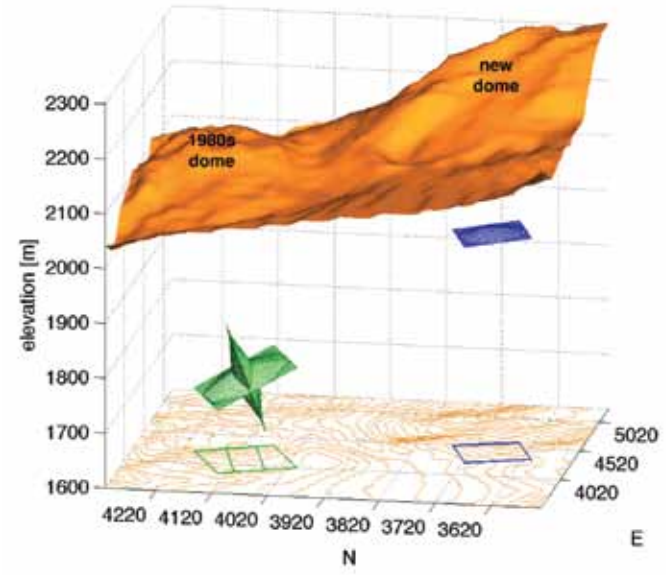

Figure 2. East-northeast, three-dimensional, perspective view of the LP crack (blue) and VLP sill-dike (green) sources. Topography is shown as a surface and is contoured on the bottom at 20 m. Distances are in m and are relative to the origin of the 20-m-grid model used to calculate Green functions.

The Seismic Story of the Nile Valley Landslide - Foreshocks, Mainshock and Aftershocks

Kate Allstadt, John Vidale, Weston Thelen, Paul Bodin *(Univ. of Washington)*

The Nile Valley landslide, in Washington State, 11 October 2009, was a translational slide involving a volume of material on the order of 10^7 cubic meters. It damaged a highway and several houses and diverted a river, causing flooding. Fortunately no one was injured because the landslide gave warning "foreshocks," - rumbling sounds, rocks raveling, and a smaller precursory landslide in the days and hours beforehand.

The "mainshock" was a complex ground failure sequence occurring over the course of about 24 hours. The more energetic events generated seismic signals that were captured by two Pacific Northwest Seismic Network (PNSN) short-period regional stations 12 and 29km away. This precise seismic timeline, in combination with detailed eyewitness reports and studies of the geology of the landslide resulted in a detailed account of the unfolding of a landslide unlike any other. This timeline is shown on Figure 1.

After the landslide occurred, we installed 16 temporary seismic stations. Despite a lack of significant continued movements, our instruments detected more than 60 small events, or "aftershocks." We were able to locate some of the larger events using beamforming techniques. The events were at the headscarp north of the slide, most likely slope failures due to instability of the newly created cliff-face.

References:

Anderson, D. and G. Taylor (2010), Nile Landslide Timeline Narrative Report, Washington State Dept of Transportation, Unpublished Report.

Acknowledgements: Thanks to the Washington State DNR and DOT, in particular to Doug Anderson and Gabe Taylor. Also to IRIS PASSCAL for lending us equipment and Agnes Helmstetter for sharing her event location methods.

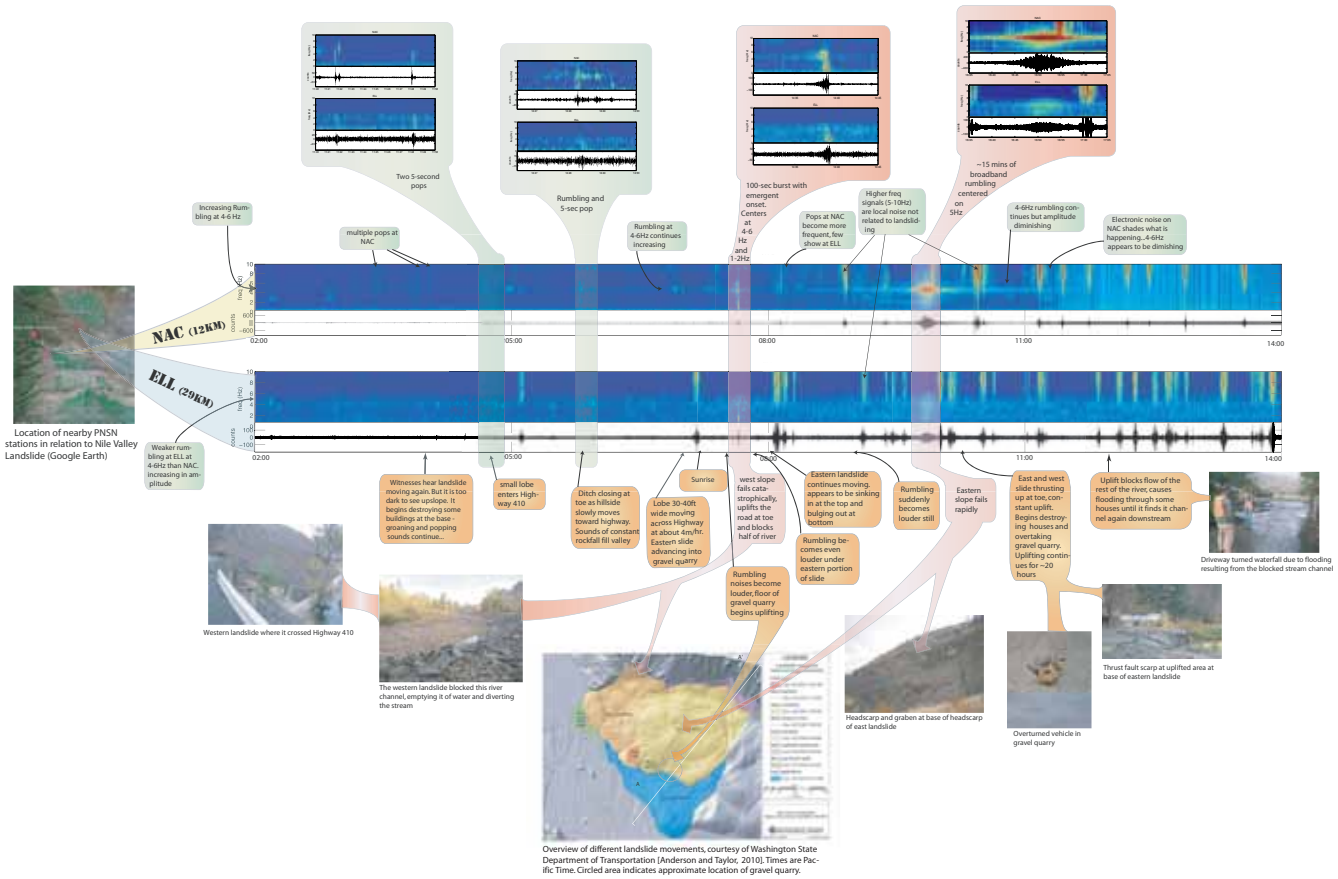

Seismic Timeline of the Nile Valley Landslide showing the main sliding sequence as detected at the two closest PNSN regional stations, both short period, vertical instruments. Station locations in relation to the slide are shown on the map at left. The spectrogram showing 12 hours of the landslide is shown on top and the traces filtered from 1 to 7Hz are shown below for each station. The seismic timeline is narrated in green at the top and the corresponding eyewitness timeline is narrated in orange at bottom. Times are Pacific Time.

A Search for the Lunar Core Using Array Seismology

Peiying Patty Lin *(Arizona State University),* **Renee Weber** *(U.S. Geological Survey),* **Edward Garnero** *(Arizona State University)*

Apollo Passive Seismic Experiment (Apollo PSE) seismometers were deployed on the nearside of the Moon between 1969 and 1972, and continuously recorded 3 components of ground motion until late 1977. These data provide a unique opportunity for investigating a planetary interior other than the Earth. PSE data potentially provide the most direct information about the structure of the lunar interior, including the thermal and compositional evolution of the Moon. The size and the state of the Moon¡¦s core remain primary questions regarding the deep lunar interior. Past seismic models of the lunar interior report significantly diminished resolution in the deepest Moon, and frequently don't cite model solutions in the deepest 500 km of the interior.

In this study, we investigate the PSE data for the presence of seismic energy that may have been reflected (or converted) from the presence of a material property contrast associated with the lunar core-mantle boundary (CMB). Borrowing from the successes of CMB imaging on Earth, we use array-stacking techniques in effort to reveal relatively low amplitude but coherent seismic signals that would otherwise be below the background noise level (noting that for the Moon, seismic coda and noise levels have been shown to be significant [*Jarosch, 1977*]. We systematically search for either P or S wave down-going energy that reflects from the CMB, with the possibility of mode conversion. The four main possibilities are PcP, ScS, ScP and PcS.

Deep moonquakes have been shown to occur and repeat in specific locations; about 65 unique clusters of deep moonquakes were identified and located by Nakamura [*2005*]. Our first processing step involved a stacking of data in each cluster [Bulow et al., 2005]. However, even in the cluster stacks, data display emergent arrivals. We thus apply a polarization filter, which is based on a product between orthogonal components of motion that enhances signals which partition onto each component, as opposed to noise. The polarized cluster stacks are then stacked a second time after time-shifting traces according to theoretical predictions of core-reflection times. This experiment, commonly referred to as double array stacking, is done for a large range of possible core radii. Preliminary analyses indicate PcP gives the most stable results, with strong evidence for a reflector at 200 km radius. ScP, while less certain, suggests an additional reflector at 330 km radius. We explore the possibility of a solid inner and fluid outer core explaining these results, a structure advocated by other methods, e.g. from laser ranging data [*Williams et al., 2006*].

References

Jarosch, H. (1977), *Bull. Seismol. Soc. Amer., 67*, 1647-1659.

Nakamura, Y. (2005), *J. Geophys. Res., 110*, doi:10.1029/2004JE002332

Bulow R.C. et al. (2005), *J. Geophys. Res., 110*, doi:10.1029/2005JE002414

Williams J. G. et al (2006), Advances in Space Research, 37, 67-71.

Acknowledgements: This research was supported by NSF grant.